AGU PUBLICATIONS

Radio Science

RESEARCH ARTICLE
10.1002/2015RS005823

Key Points:
- Thermospheric acoustic gravity wave activity over Wallops Island is studied
- Precise spectral calculations are performed in the presence of significant data gaps
- The altitude variation of the gravity wave spectrum is analyzed

Correspondence to:
C. Negrea,
Catalin.negrea@noaa.gov

Citation:
Negrea, C., and N. A. Zabotin (2016), Mean spectral characteristics of acoustic gravity waves in the thermosphere-ionosphere determined from Dynasonde data, *Radio Sci.*, *51*, 213–222, doi:10.1002/2015RS005823.

Received 6 OCT 2015
Accepted 25 FEB 2016
Accepted article online 3 MAR 2016
Published online 30 MAR 2016

Mean spectral characteristics of acoustic gravity waves in the thermosphere-ionosphere determined from Dynasonde data

Cătălin Negrea[1,2,3,4] and Nikolay A. Zabotin[1,2]

[1]Department of Electrical, Computer and Energy Engineering, University of Colorado Boulder, Boulder, Colorado, USA, [2]Cooperative Institute for Research in Environmental Sciences, University of Colorado Boulder, Boulder, Colorado, USA, [3]Space Weather Prediction Center, National Oceanic and Atmospheric Administration, Boulder, Colorado, USA, [4]Institute of Space Science, Magurele, Romania

Abstract Wave-like disturbances have been observed in the ionospheric plasma for several decades using a wide range of remote sensing techniques. In this paper, the use of Dynasonde-derived ionospheric "tilt" measurements is demonstrated to determine the dominant features of the underlying acoustic gravity wave spectrum and its height variation. The diurnal ionospheric variability introduces data gaps of varying length and distribution at any constant height level. This excludes the use of conventional fast Fourier transform techniques for spectral calculations. To obtain a complete and accurate image of the height variability of the wave activity in the thermosphere-ionosphere, a method is required that would provide physically comparable results at all altitudes, regardless of the variations in sampling. In addition, the true geophysical variability should be distinguished from overlapping noise. The proposed solution is a combination of the well-known Lomb-Scargle and Welch methods, with the dataset of interest being divided into several overlapping subintervals and the mean spectrum calculated using results for those subintervals for which the power spectral density integral equals the time domain variance within a preset tolerance. The choice of the tolerance value is justified by means of numerical simulations using synthetic data similar to the tilt measurements. The proposed method is verified using a 10 day long dataset obtained with the Wallops Island Dynasonde. Results obtained with this method are compared in this paper with those obtained with a basic implementation and with a filtering method based on the amount of available data. A considerable reduction in the number of artifacts is observed with the use of this innovative approach, allowing reliable conclusions to be derived regarding the acoustic gravity wave spectrum and its height variability.

1. Introduction

An unprecedented amount of ionospheric data has become available in recent years from ground-based radars compatible with the Dynasonde method. This study aims to demonstrate the possibility of using Dynasonde data for the study of the dominant gravity wave spectrum in the thermosphere-ionosphere while also presenting an innovative method of estimating the mean power spectral density (PSD) of a time series containing data gaps. It has previously been demonstrated that Dynasonde tilt data can be used to fill the existing gap in tidal measurements in the thermosphere-ionosphere [*Negrea et al*., 2015]. The part of the spectrum associated with acoustic gravity waves (AGW) is thought to have smaller amplitude, while it is also fairly smooth (no dominant spectral harmonics, such as that associated with the diurnal tide) and continuous over time periods covering several days or more [e.g., *Djuth et al*., 2010]. Recent work into estimating the PSD of a time series that does not contain high-amplitude harmonics has shown that this is difficult even if small data gaps are present (C. Munteanu, C. Negrea, M. Echim, and K. Mursula, Effect of data gaps: Comparison of different spectral analysis methods, submitted to *Annales Geophysicae*, 2015).

The estimation of the PSD associated with a time series is a general problem encountered in many branches of science. For the case of a uniformly sampled signal, the problem is trivial and immediately addressed by use of the well-known fast Fourier transform algorithm (FFT). However, in many cases the data series contains gaps of varying size and disposition. For the particular case of Dynasonde data, the normal diurnal variability of the ionosphere introduces significant data gaps at most altitudes. More advanced methods can be used to estimate the PSD of such time series. One frequently used is the Lomb-Scargle method [*Lomb*, 1976; *Scargle*, 1982, 1989; *Press and Rybicki*, 1989; *Hocke*, 1998; *Hocke and Kämpfer*, 2009]. However, no universally valid method is known to determine an orthogonal frequency set for a nonuniformly sampled time series.

Because the frequency set is not orthogonal, the power contained in a given frequency band is not independent of the effective power contained in other frequency bands. This causes a multitude of possible errors that are difficult to diagnose based purely on theoretical considerations.

The AGW spectrum is known to be highly variable in the thermosphere-ionosphere and is generally observed using the induced traveling ionospheric disturbances (TIDs) as tracers. The presence of TIDs can impact GPS accuracy [*Hernandez-Pajares et al.*, 2006], and their eventual dissipation can change the effect the background neutral winds [*Yigit et al.*, 2009; *Vadas et al.*, 2014] and the spectrum of tidal waves [*Walterscheid et al.*, 1987; *Vadas et al.*, 2014]. Despite the availability of data obtained with several remote sensing techniques, Super Dual Auroral Radar Network (SuperDARN) [*Bristow et al.*, 1996], incoherent scatter radar (ISR) [*Nicolls and Heinselman*, 2007; *Nicolls et al.*, 2014], GPS total electron content (TEC) [*Kotake et al.*, 2006], and 630 nm airglow imagers [*Shiokawa et al.*, 2003], the existing knowledge regarding the TID spectrum is constrained by either limited temporal coverage or a limited altitude range and lack of height-stratified data.

The goal here is to extract the dominant mean wave spectrum characterizing time intervals of at least several days and over a wide altitude range, using the Dynasonde tilt measurements at Wallops Island, VA. In such cases, the Welch method is typically used [*Welch*, 1967], splitting the available data into a number of overlapping subintervals. Under the assumption that the dominant variability has Gaussian statistics, averaging the power spectra obtained for all subintervals would yield the mean power spectrum characterizing the entire dataset.

The proposed method is a combination of the Lomb-Scargle and Welch methods, where for each subinterval a PSD is calculated using a Lomb-Scargle implementation and subintervals for which the time domain variance does not equal the PSD integral within a reasonable uncertainty are discarded. While the focus here is on ionospheric data and the AGW spectrum, the method we propose is based on fundamental principles and as such it is applicable to a variety of data types.

The paper is structured as follows: Section 2 discusses the difficulties introduced by the natural ionospheric variability and describes the proposed solution. In section 3, an estimate of the error introduced by the presence of noise superimposed onto the intended signal is determined. Section 4 shows the results of this method when processing real ionospheric tilt data and compares this result with those obtained using two other possible approaches. Finally, section 5 contains conclusions and a brief discussion.

2. Dynasonde Data

The data used are a 10 day long dataset from 2 October to 11 October 2013, obtained using the Vertical Incidence Pulsed Ionospheric Radar (VIPIR) radar system at Wallops Island, VA [*Grubb et al.*, 2008], at a 2 min cadence, allowing for the study of waves with frequencies of up to 4.14 mHz. The raw data were processed using the software analysis package based on Dynasonde principles [*Paul et al.*, 1974; *Wright and Pitteway*, 1979, 1982, 1999; *Wright et al.*, 1980; *Pitteway and Wright*, 1992], a component of which is the NeXtYZ inversion procedure [*Zabotin et al.*, 2006]. The results are the parameters of the wedge stratified ionosphere model (WSI), which describes the local 3-D electron density distribution. The model assumes a series of electron densities N_{ei} at a series of heights h_i along the vertical axis, with the added feature that each electron density value corresponds to a portion of a slant plane. The electron density in the region between two adjacent planes (which has the shape of a wedge) depends monotonically on the ratio of distances to the planes. The horizontal components n_x, n_y of the normal vector of each plane are referred to as "tilts," rigorously defined as

$$\boldsymbol{n} = \left(n_x, n_y, n_z\right) = \frac{\nabla N_e}{|\nabla N_e|} \tag{1}$$

The resulting outputs are a set of height profiles of electron density X (west-east) and Y (south-north) tilts and Doppler velocity height-stratified profiles. The focus of this work is the tilt data, since this parameter is ideal for the study of wave activity for several reasons. First, a wave propagating through the thermospheric gas that induces a wave-like variation of the local electron density [*Fritts and Alexander*, 2003; *Nicolls et al.*, 2014]

$$N_e(t) = N_{e0}\, e^{i(\boldsymbol{k}\cdot\boldsymbol{r}-\omega t)} \tag{2}$$

must necessarily produce a wave-like variation of the tilts

$$n_{x,y} = \frac{k_{x,y}}{|\nabla N_e|} N_{e0}\, e^{i(\boldsymbol{k}\cdot\boldsymbol{r}-\omega t)} \tag{3}$$

where N_{e0} is the amplitude of the wave with ground-based angular frequency $\omega = \omega_0 - \boldsymbol{u}\cdot\boldsymbol{k}$, ω_0 is the intrinsic wave frequency, $\boldsymbol{k} = (k_x, k_y, k_z)$ is the wave vector, $\boldsymbol{u}$ is the neutral wind vector, $\boldsymbol{r}$ is the position vector, and t is

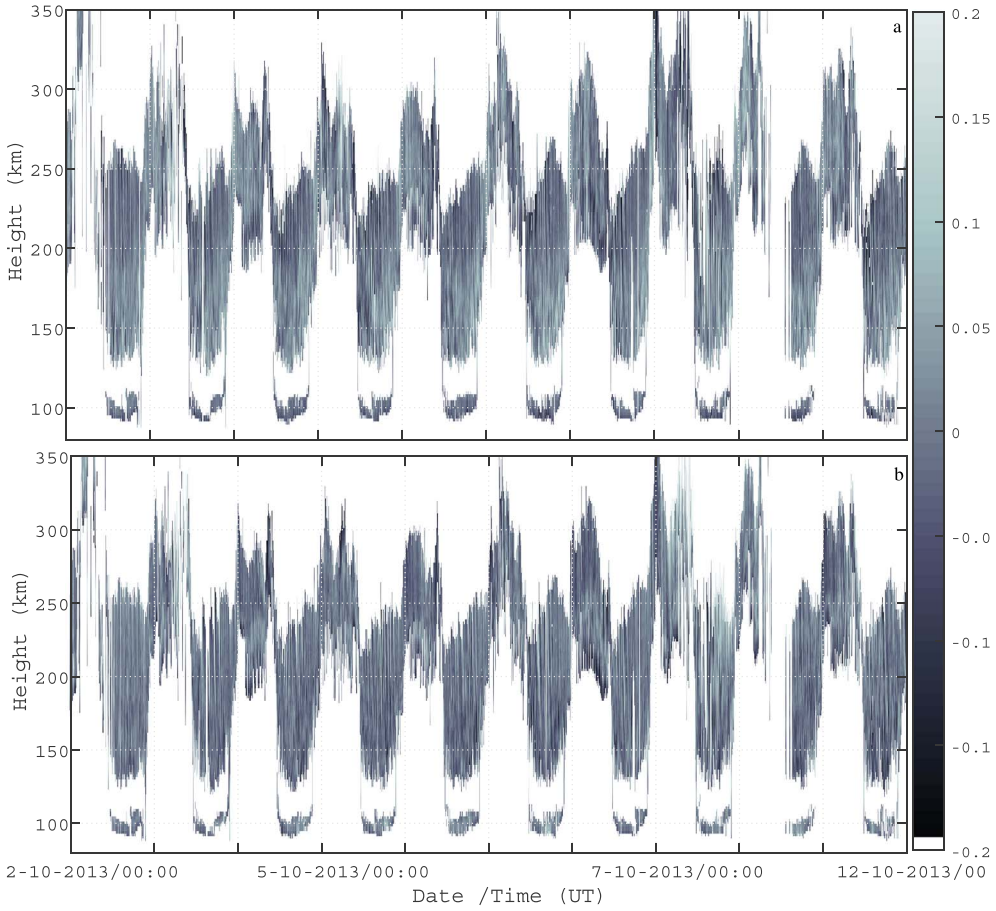

Figure 1. Temporal and altitude variability of the (a) west-east and (b) south-north tilt data. The dataset was obtained at Wallops Island, VA, and it covers the time interval from 2 October to 11 October 2013.

the time. Second, the two tilt components provide differentiation between waves propagating in different directions through the $k_{x,y}$ term in equation (3). While the tilt measurements are currently unique to the Dynasonde technique, they are unambiguously related to the horizontal components of the electron density gradient, which has been previously used to determine the parameters associated with gravity-wave-induced TIDs [*Oliver et al*., 1994; *Oliver et al*., 1995].

Figure 1 shows the entire tilt data obtained at Wallops Island within the 10 day interval (2–11 October 2013). Note the variability of the altitude coverage of the data, with the day-to-night and the night-to-day transitions as a prominent feature. A more detailed image is necessary to highlight the individual wave signatures in the data. Figure 2 shows the *X* and *Y* tilt data covering only 24 h during 5 October 2013. Here the slightly inclined wave fronts (indicating downward phase propagation) characteristic of AGWs are clearly visible throughout most of the interval, with the dominant waves characterized by periods ranging from several minutes to a few hours.

3. Lomb-Scargle Method

Both Figures 1 and 2 show that at any given altitude, there is a nonuniformly sampled time series when considering periods of several days. An average power spectrum characterizing these data can be obtained by using the Lomb-Scargle method. The latter is essentially an implementation of the least squares fit that yields the power spectrum $P(f)$ associated with a given time series as

$$P(f) = \frac{1}{N}\left[\frac{(\Sigma_i(x_i - \overline{x})\ \cos\omega(t_i - \tau))^2}{\Sigma_i \cos^2\omega(t_i - \tau)} + \frac{(\Sigma_i(x_i - \overline{x})\ \sin\omega(t_i - \tau))^2}{\Sigma_i \sin^2\omega(t_i - \tau)}\right] \quad (4)$$

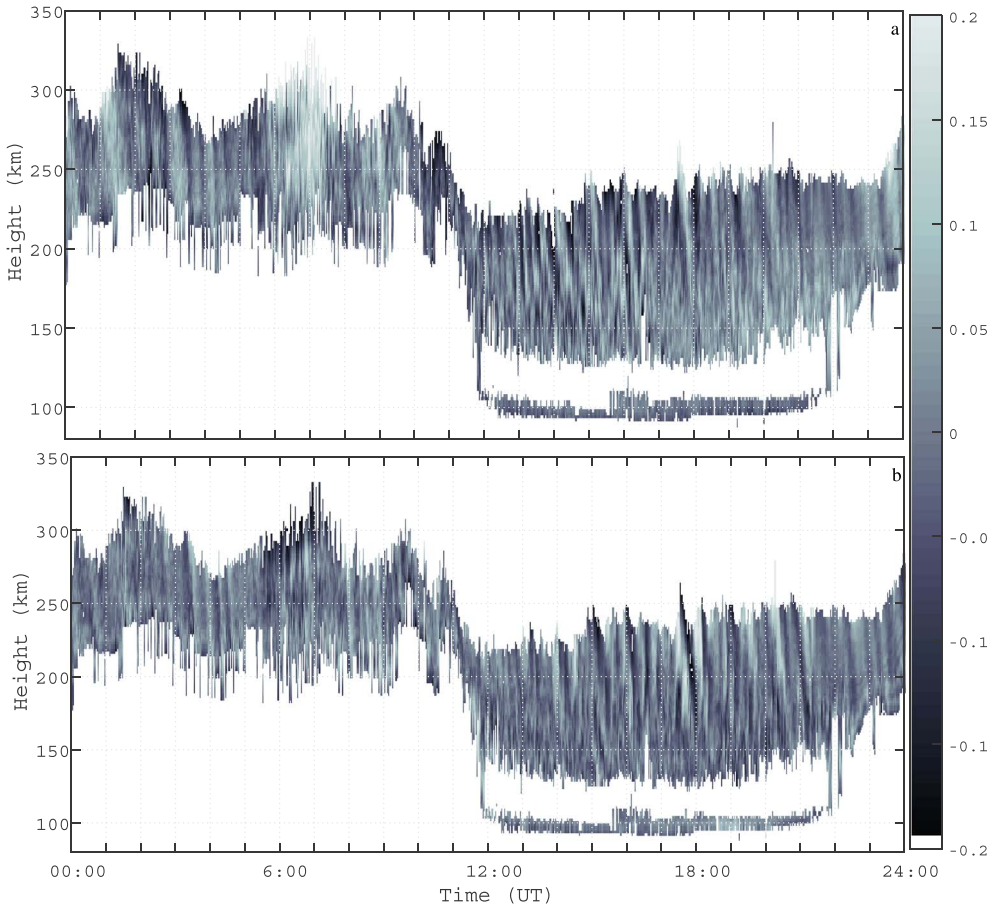

Figure 2. Same as Figure 1 but covering only 24 h on 5 October 2013. The slightly inclined strips are indicative of the phase fronts created by upward propagating AGWs.

with the parameters $\overline{x} = \frac{1}{N}\sum x_i$, $\tan(2\omega\tau) = \frac{\sum_i \sin 2\omega t_i}{\sum_i \cos 2\omega t_i}$, $\omega = 2\pi f$ is the angular frequency, and N is the size of the dataset (t_i, x_i). The method is widely used for spectral analysis of nonuniformly sampled data in a variety of scientific fields [*Horne and Baliunas*, 1986; *Schimmel*, 2001; *Thong et al*., 2004; *Zhou et al*., 1997].

Results of spectral calculations performed with a large time series can be subject to significant variations. Additional complications may be caused by inevitable noise in the data. Assuming that this noise has a zero mean, the approach described by *Welch* [1967] can be used to mitigate the problem. The Welch method is used to determine the mean PSD by dividing the data into overlapping subintervals, calculating the PSD for each subinterval, and finally averaging results for all subintervals. This approach is typically used with a FFT implementation, but using the technique in conjunction with the Lomb-Scargle method is perfectly valid.

As shown by Munteanu et al. (submitted manuscript, 2015), existing spectral analysis techniques suffer from higher errors and biases in the presence of extensive data gaps. These caveats can be negligible if the spectral features of interest are very high amplitude and narrow bandwidth, such as tidal harmonics [*Negrea et al*., 2015], and it may also be possible to impose frequency-dependent criteria to determine the validity of such peaks [*Baluev*, 2008]. For the frequency range affected by thermospheric AGWs, the mean amplitudes over longer time intervals are generally smaller than those of tidal modes. In contrast, the associated bandwidth is much larger and the overall shape of the spectrum smoother. Tests performed by Munteanu et al. (submitted manuscript, 2015) using data characterized by a similarly "smooth" spectrum have shown that if more than 10–20% of the entire time series is removed, the resulting error in the final result is significant and frequency dependent, leading to a spectrum that is deformed when compared to the expected result.

In the case of the AGW spectrum, applying a filtering criterion of statistical significance would exclude most of the wave activity characterized by smaller amplitudes. The approach suggested here uses an integral

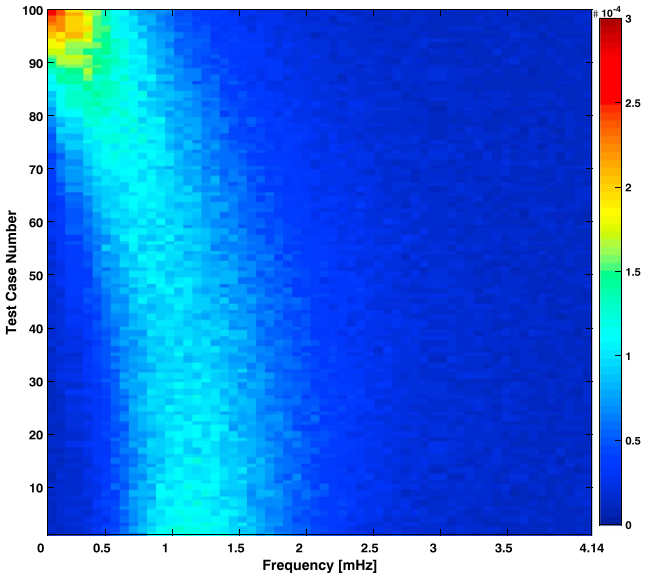

Figure 3. Power spectra characterizing the synthetic datasets. The dominant structure is similar to that produced due to the height variation of the AGW spectrum. The fine granular structure is due to the added noise term in equation (7).

criterion to establish the validity of a whole PSD as opposed to individual harmonics. For a dataset characterized by a stationary spectrum and with minimal or no noise, the PSD must follow the identity

$$\Sigma_1^{N_f} P_i \cdot (t_N - t_1) \cdot \Delta f_i = \sigma^2 \quad (5)$$

where P_i is the power calculated for frequency bin Δf_i using equation (4), N_f is the total number of frequency bins, $t_N - t_1$ is the length of the time interval considered, and σ^2 is the variance in the time domain.

4. Synthetic Data Testing

In the case of real data, equation (5) is fulfilled only approximately

$$\Sigma_1^{N_f} P_i \cdot (t_N - t_1) \cdot \Delta f_i + \xi = \sigma^2 \quad (6)$$

where the extra term ξ sums up the effect due to noise and nonstationarity and for our purposes can be interpreted as an error. To determine an upper boundary for ξ, a test has been devised using synthetic data.

One hundred synthetic time series have been generated using an amplitude spectrum $A(f)$ that follows a gamma distribution:

$$A(f) = \sqrt{\frac{2}{N} P(f)} = A_0 \cdot F(f, \alpha, \beta) + B_0 \quad (7)$$

where $F(f, \alpha, \beta) = \frac{1}{\left(\int_0^\infty x^{\alpha-1} e^{-\alpha} \mathrm{d}\alpha\right) \beta^\alpha} f^{\alpha-1} e^{-\frac{f}{\beta}}$ is the standard gamma probability density function, α is the shape parameter, varying from 1.05 to 4.8, and β is the scale parameter, varying from $3 \cdot 10^{-4}$ to $6.5 \cdot 10^{-4}$. A further scaling factor A_0 of $1.1 \cdot 10^{-5}$ and a uniform background level B_0 of $3.5 \cdot 10^{-3}$ are applied. The time series equivalent to this spectrum is determined, and, finally, the resulting "dataset" is "polluted" using Gaussian distributed noise with mean zero and $2 \cdot 10^{-2}$ variance. The resulting datasets each contain 7200 points and are intended to mimic the expected thermospheric AGW spectrum, with the added noise component also introducing a degree of nonstationarity. Figure 3 shows the full set of PSDs characterizing the synthetic datasets.

The time series generated for each test case is separated into subintervals 120 points long, with a 10-point overlap. For each subinterval, both the time domain variance and the PSD integral are calculated and the relative error $\Delta\xi = \left(\Sigma_1^{N_f} P_i \cdot (t_N - t_1) \cdot \Delta f_i - \sigma^2\right)/\sigma^2$ is determined. Figure 4 shows the maximum value for $\Delta\xi$ obtained in any of the 65 subintervals in each test case. The values tend to locate between 2 and 4%, with a number of four outliers approaching 5%. For the purpose of our calculations with Dynasonde tilt data, based on the results shown in Figure 4, a maximum acceptable value of $\xi_0 = 0.04 \cdot \sigma^2$ for ξ will be used to determine the validity of individual subintervals. Assuming a Gaussian distribution to the values of $\Delta\xi$, the chosen 4% value encompasses 96% of the obtained values or approximately double the standard deviation.

5. Results With Nonuniformly Sampled Dynasonde Data

Determining the correct power spectrum is essential for understanding the AGW properties in the thermosphere-ionosphere and their subsequent impact. Because of the very different sampling throughout the altitude range of interest, it is essential that results at different heights be equivalent in their physical

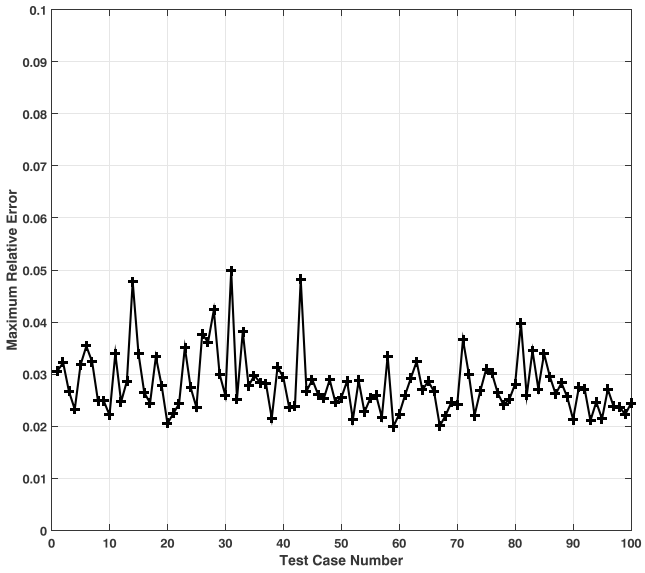

Figure 4. Maximum percent error obtained for each test case using a subinterval size of 120 points. The majority of the values are between 0.02 and 0.04, with four outliers closer to 0.05. Based on this result, a value of $\xi_0 = 0.04 \cdot \sigma^2$ is chosen as the maximum accepted error.

meaning. This is accomplished by using the method described in section 3 with an added oversampling factor of 10 [*Press et al.*, 1992], in conjunction with the threshold of 4% on $\Delta\xi$, as obtained in section 4. To highlight the importance of filtering and of the derived criterion, the tilt power spectrum is calculated for the selected 10 day dataset in October 2013 using three methods. First this is achieved using our proposed approach; second, this is done with a filtering criterion based solely on the size of the data gaps and, third, with no filtering at all. In all three cases, the subinterval length was 4 h with an overlap of 20 min between adjacent subintervals.

Figure 5 shows the *X* tilt power spectra corresponding to the data shown in Figure 1. No filtering criteria were imposed, and as such, the averaging was performed using results for all subintervals that contained a minimum of 10 data points. The resulting average spectra contain several questionable features, such as the sudden changes in the background level around 210, 240, and 260 km. Below 150 km, the decrease in the number of subintervals causes an increase in the noise level, making interpretation difficult. Using this result, one could erroneously arrive at the conclusion that the waves propagating from lower altitudes are steadily attenuated as they reach higher altitudes but have a higher level of wave activity between 210 and 240 km and above 260 km. This would imply some wave sources that are not directly linked to typical forcings in the lower atmosphere, a situation that, while possible, is highly unlikely. Since the buoyancy frequency decreases with altitude in the thermosphere, the highest intrinsic frequency at which nonevanescent gravity waves may exist also decreases with altitude.

Imposing a filtering criterion that is entirely based on the amount of data available produces better results, as can be observed in Figure 6. In this case, the mean spectrum was obtained using only those subintervals that contained a minimum of 80% of the ideal number of data points. The apparent quality of the result in Figure 6 is better than that in Figure 5, with some of the questionable features removed. Note that the overall height variation of the spectra is similar in the two figures, but the fine structure is more clearly defined in Figure 6. The background level above 260 km is again higher than that observed immediately below 260 km. This appears unrealistic, since the buoyancy frequency decreases with altitude, which would prevent the effective propagation of high-frequency components of the spectrum. It is much more likely that this is an artifact caused by the limited amount of data available above 260 km: the impact of a small number

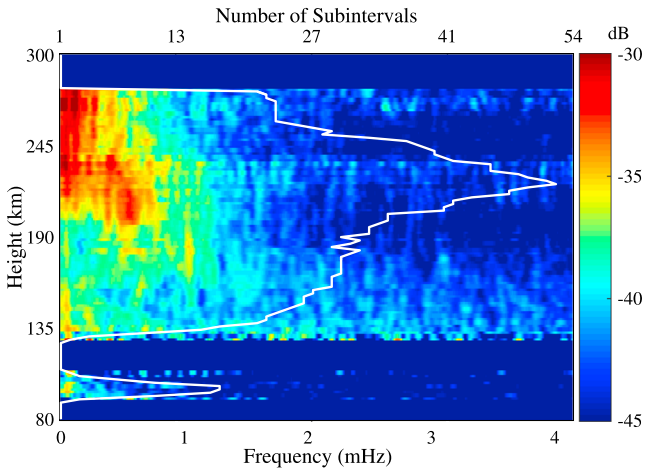

Figure 5. *X* tilt power spectra calculated using the Lomb-Scargle and Welch methods, with no restrictions on the number of points per subintervals and power spectral density integral. The superimposed white line shows the number of subintervals that were used at each altitude to calculate the mean power spectra.

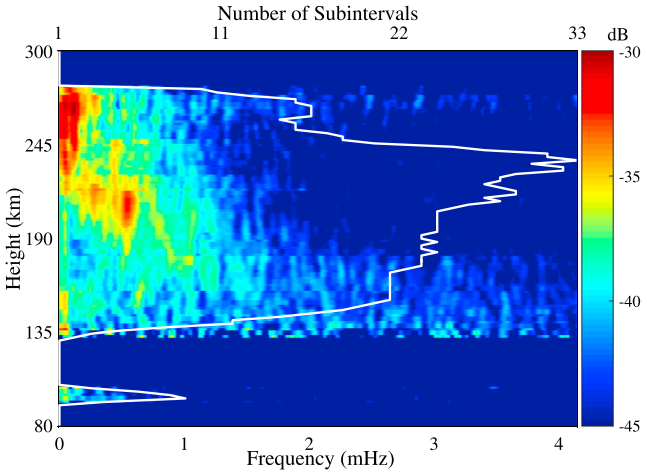

Figure 6. *X* tilt power spectra calculated using the Lomb-Scargle and Welch methods, discarding subintervals with less than 80% of the ideal number of points. The superimposed white line shows the number of subintervals that were used at each altitude to calculate the mean power spectra.

of erroneous spectra is augmented as the number of valid subintervals decreases. A threshold could be imposed to discard results calculated using a smaller number of subintervals. However, such a criterion could be somewhat subjective.

Finally, Figures 7 and 8 show the *X* and *Y* tilt power spectra calculated using our proposed method with a 4% threshold imposed on $\Delta\xi$. This approach has the starting advantage of being based on fundamental theoretical principles that remove the possible impact of subjectivity and assure that results obtained at different altitudes, times, and locations can be used for quantitative comparisons. Figure 7, when compared to Figures 5 and 6, is in much better agreement with existing knowledge on the height dependence of the AGW spectrum [e.g., *Djuth et al.* [2010]]. Note that as the number of subintervals in Figures 7 and 8 approaches 1, the results become noisier. This is because in these cases our method reduces to the classic Lomb-Scargle method, without the added noise reduction of the Welch method.

The approach proposed in this study produces a set of power spectra without introducing height-dependent artifacts while reducing noise as much as possible, allowing for valuable information on the average AGW activity to be obtained. At Wallops Island, for the time interval from 2 October to 11 October 2013, the height dependence of the wave spectrum is characterized by the slant shape, as can be observed in Figures 7 and 8, with the peak frequency of observed waves decreasing with height. Note that conclusions about maximum/minimum observed frequency can be biased by the choice of the dynamic range of the color scale, which is only 15 dB for these illustrations. Due to the natural ionospheric variability, the height interval from 80 km up to 220–240 km is mostly indicative of daytime wave activity, and the height interval from 220–240 to 280 km is mostly indicative of nighttime wave activity. A broadband maximum in the spectrum of both tilts is observed between 180 and 220–230 km and at frequencies between 0.1 and 0.8 mHz. A second maximum is observed in the *X* tilt spectrum between 220 and 280 km at frequencies below 0.2 mHz. This implies a transfer of energy from waves with periods of several tens of minutes to waves with periods of more than 1 h as we move up in the altitude. This is likely due to nonlinear interactions [*Angelats i Coll and Forbes*, 2002] in addition to energy transfer from AGWs to the mean thermospheric flow and wave reflection due to critical layers [*Vadas*, 2007, *Godin*, 2014]. The higher spectral amplitudes more abundant in Figure 7 indicate a preferred direction of propagation in the horizontal plane along the west-east axis. This appears to be more pronounced above 220 km. The propagation directions of gravity waves are known to vary significantly with season and geographical position, and different results may be obtained for a different Dynasonde station or time of year.

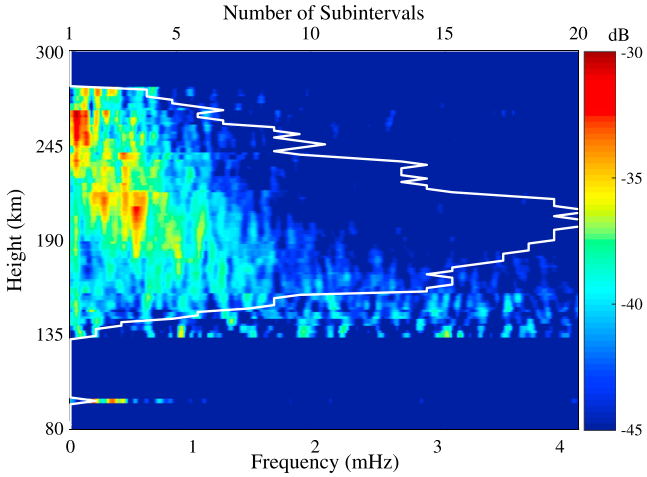

Figure 7. *X* (south-north) tilt power spectra calculated using the Lomb-Scargle and Welch methods, with a maximum tolerable error, $\Delta\xi$ of 4%. The superimposed white line shows the number of subintervals that were used at each altitude in order to calculate the mean power spectrum.

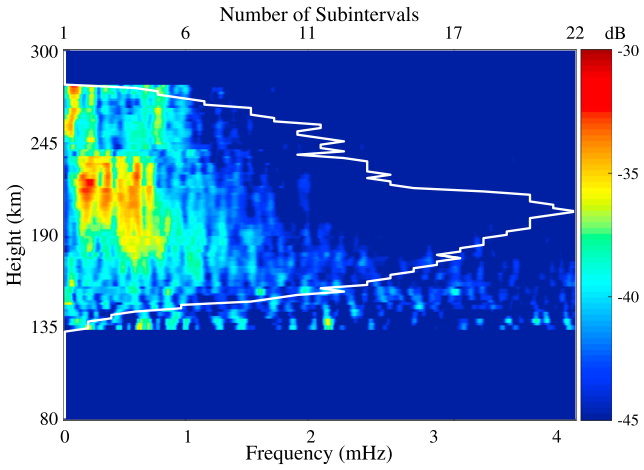

Figure 8. Same as Figure 7 but for *Y* (west-east) tilt data.

6. Conclusions and Discussion

This study has shown that Dynasonde tilt measurements are an extremely valuable resource for the study of acoustic gravity wave activity in the thermosphere-ionosphere. Due to the natural variability of the ionosphere, an example of which is shown in Figure 1, traditional approaches for the calculation of the power spectra are unsuitable. The limitations of the more advanced Lomb-Scargle method are discussed, and a method is presented that circumvents problems due to data gaps, noise, and nonstationarity. A given time series is divided into several overlapping subintervals, with a Lomb-Scargle derived spectrum calculated for each subinterval. The mean spectrum representative of the entire time series is obtained by averaging results for those subintervals, for which the power spectral density integral is equal to the variance in the time domain, within a reasonable tolerance.

To quantify the term "reasonable tolerance," 100 synthetic datasets are used. It has been shown that even in the absence of data gaps, the term ξ in equation (6) is not necessarily zero. By analyzing the distribution of the maximum discrepancies for all of the 100 test cases, a value of 4% is obtained as the reasonable value for the relative tolerance $\Delta\xi$. This is then applied to spectral calculations with real tilt data obtained at Wallops Island between 2 October and 11 October 2013. Results obtained using this method (Figures 7 and 8) are compared to those obtained without filtering (Figure 5) and with a filtering based on the size of the data gaps (Figure 6). The proposed approach provides clean and smooth results revealing largely expected properties of the thermospheric wave activity. For example, the peak frequency in the spectra decreases with the altitude indicating a transfer of energy from waves with periods of tens of minutes to waves with periods of more than 1 h.

The fundamental assumptions behind equations (5) and (6) require some discussion. Under ideal conditions, the integral over the entire PSD must equal the time domain variance. In practice, the integral is performed over a limited bandwidth, in this case covering periods from 4 min to 4 h. At ionospheric altitudes, the diurnal, semidiurnal, and terdiurnal tidal modes constitute an additional source of variability. Since the periods of tidal modes are 24, 12, and 8 h, respectively, their contributions are not included in the sum on the left-hand side of equations (5) and (6), while the impact on the actual ionospheric variability is present. Using a window of larger size is not desirable due to the high variability of the AGW spectrum that would result in much higher values for ξ_0. The net effect is that results for some subintervals may be discarded if the tidal amplitudes are significant when compared to the total AGW activity. However, this is unlikely to be a systematic problem: the bandwidth occupied by the tidal harmonics is infinitesimal in comparison to that occupied by the AGW spectrum, and their resulting contribution to the PSD integral is generally small.

Finally, a remark on the general validity of the results obtained in section 4 is needed. The value $\xi_0 = 0.04 \cdot \sigma^2$ and the results in Figure 4 are partially dependent on the specifics of the synthetic datasets used (through the parameters in equation (7)). The values chosen here were intended to produce a dataset with characteristics similar to those found in Dynasonde-derived tilt data. While this method is generally valid and applicable to any type of data, the value of 4% for $\Delta\xi$ may not be. Determining an appropriate value for different applications is possible by following the methodology outlined by us in section 4, with a suitable expression for $A(f)$.

The innovative method described here provides good spectral estimates in the presence of extensive data gaps. Starting from Dynasonde-derived tilt measurements, the AGW spectrum can be correctly obtained and its variation with altitude observed. The method is based on fundamental principles of spectral analysis and has a wide applicability for other types of data characterized by similarly smooth power spectra.

Acknowledgments
This work was supported by the Office of Naval Research Basic Research Challenge program, award N000141310348, and by the European Community's Seventh Framework Programme (FP7/2007–2013) under grant agreement 313038 (STORM), and a grant of the Romanian Ministry of National Education, CNCSUEFISCDI, project PN-II-ID-PCE-2012-4-0418. Authors are grateful to Dr. T.W. Bullett for his effort on supporting the Wallops Dynasonde system. Field support of Wallops Dynasonde operation has been provided, in part, by the staff of the NASA's Wallops Flight Facility. The Dynasonde data are accessible through the project's website (http://surf.colorado.edu) upon request to the author (N.Z.) as well as through NGDC's MIRRION server (ftp://ftp.ngdc.noaa.gov/ionosonde/data/WI937/). This work utilized the University of Colorado Boulder research computing facility, which is supported by the National Science Foundation (award number CNS-0821794).

References

Angelats i Coll, M., and J. M. Forbes (2002), Nonlinear interactions in the upper atmosphere: The $s = 1$ and $s = 3$ non-migrating semidiurnal tides, *J. Geophys. Res.*, *107*(A8), 1157, doi:10.1029/2001JA900179.

Baluev, R. V. (2008), Assessing statistical significance of periodogram peaks, *Mon. Not. R. Astron. Soc.*, *385*(3), 1279–1285, doi:10.1111/j.1365-2966.2008.12689.x.

Bristow, W. A., R. A. Greenwald, and J. P. Villain (1996), On the seasonal dependence of medium-scale atmospheric gravity waves in the upper atmosphere at high latitudes, *J. Geophys. Res.*, *102*, 11,585–11,595, doi:10.1029/97JA00515.

Djuth, F. T., L. D. Zhang, D. J. Livneh, I. Seker, S. M. Smith, M. P. Sulzer, J. D. Mathews, and R. L. Walterscheid (2010), Arecibo's thermospheric gravity waves and the case for an ocean source, *J. Geophys. Res.*, *115*, A08305, doi:10.1029/2009JA014799.

Fritts, D. C., and M. J. Alexander (2003), Gravity wave dynamics and effects in the middle atmosphere, *Rev. Geophys.*, *41*(1), 1003, doi:10.1029/2001RG000106.

Godin, O. A. (2014), Dissipation of acoustic-gravity waves: An asymptotic approach, *J. Acoust. Soc. Am.*, *136*(6), doi:10.1121/1.4902426.

Grubb, R. N., R. Livingston, and T. W. Bullett (2008), A new general purpose high performance HF Radar, *Proc.*, XXIX URSI General Assembly, Chicago, Il.

Hernandez-Pajares, M., J. M. Juan, and J. Sanz (2006), Medium-scale traveling ionospheric disturbances affecting GPS measurements: Spatial and temporal analysis, *J. Geophys. Res.*, *111*, A07S11, doi:10.1029/2005JA011474.

Hocke, K. (1998), Phase estimation with the Lomb-Scargle periodogram method, *Ann. Geophys.*, *16*(3), 356–358.

Hocke, K., and N. Kämpfer (2009), Gap filling and noise reduction of unevenly sampled data by means of the Lomb-Scargle periodogram, *Atmos. Chem. Phys.*, *9*, 4197–4206, doi:10.5194/acp-9-4197-2009.

Horne, J. H., and S. L. Baliunas (1986), A prescription for period analysis of unevenly sampled time series, *Astrophys. J.*, *302*, 757–763, doi:10.1086/164037.

Kotake, N., Y. Otsuka, T. Tsugawa, T. Ogawa, and A. Saito (2006), Climatological study of GPS total electron content variations caused by medium-scale traveling ionospheric disturbances, *J. Geophys. Res.*, *111*, A04306, doi:10.1029/2005JA011418.

Lomb, N. R. (1976), Least-squares frequency analysis of unequally spaced data, *Astrophys. Space Sci.*, *39*, 447–462, doi:10.1007/BF00648343.

Negrea, C., N. Zabotin, T. Bullett, M. Codrescu, and T. Fuller-Rowell (2015), Ionospheric response to tidal waves measured by Dynasonde techniques, *J. Geophys. Res. Space Physics*, *120*, doi:10.1002/2015JA021574.

Nicolls, M. J., and C. J. Heinselman (2007), Three-dimensional measurements of traveling ionospheric disturbances with the Poker Flat Incoherent Scatter Radar, *Geophys. Res. Lett.*, *34*, L21104, doi:10.1029/2007GL031506.

Nicolls, M. J., S. L. Vadas, N. Aponte, and M. P. Sulzer (2014), Horizontal parameters of daytime thermospheric gravity waves and *E* region neutral winds over Puerto Rico, *J. Geophys. Res. Space Physics*, *119*, 575–600, doi:10.1002/2013JA018988.

Oliver, W. L., S. Fukao, Y. Yamamoto, T. Takami, M. D. Yamanaka, M. Yamamoto, T. Nakamura, and T. Tsuda (1994), MU radar observations of ionospheric density gradients produced by gravity wave packets, *J. Geophys. Res.*, *99*, 6321–6329, doi:10.1029/94JA00171.

Oliver, W. L., S. Fukao, M. Sato, Y. Otsuka, T. Takami, and T. Tsuda (1995), Middle and upper atmosphere radar observations of the dispersion relation for ionospheric gravity waves, *J. Geophys. Res.*, *100*(A12), 23,763–23,768, doi:10.1029/95JA02520.

Paul, A. K., J. W. Wright, and L. S. Fedor (1974), The interpretation of ionospheric radio drift measurements-VI. Angle-of-arrival and group path [echolocation] measurements from digitized ionospheric soundings: The group-path vector, *J. Atmos. Sol. Terr. Phys.*, *36*(2), 93–214, doi:10.1016/0021-9169(74)90040-3.

Pitteway, M. L. V., and J. W. Wright (1992), Toward an optimum receiving array and pulse set for the Dynasonde, *Radio Sci.*, *27*(4), 481–490, doi:10.1029/92RS00269.

Press, W. H., and G. B. Rybicki (1989), Fast algorithm for spectral analysis of unevenly sampled data, *Astrophys. J.*, *338*, 277–280, doi:10.1086/167197.

Press, W. H., S. A. Teukolsky, W. T. Vetterling, and B. P. Flannery (1992), *Numerical Recipes in Fortran*, 2nd ed., Cambridge Univ. Press, Cambridge.

Scargle, J. D. (1982), Studies in astronomical time series analysis. II. Statistical aspects of spectral analysis of unevenly spaced data, *Astrophys. J.*, *263*, 835–853, doi:10.1086/160554.

Scargle, J. D. (1989), Studies in astronomical time series analysis. III. Fourier transforms autocorrelation functions and cross-correlation functions of unevenly spaced data, *Astrophys. J.*, *343*, 874–887, doi:10.1086/167757.

Schimmel, M. (2001), Emphasizing difficulties in the detection of rhythms with Lomb-Scargle periodograms, *Biol. Rhythm Res.*, *32*(3), 341–346, doi:10.1076/brhm.32.3.341.1340.

Shiokawa, K., C. Ihara, Y. Otsuka, and T. Ogawa (2003), Statistical study of nighttime medium-scale traveling ionospheric disturbances using midlatitude airglow images, *J. Geophys. Res.*, *108*(A1), 1052, doi:10.1029/2002JA009491.

Thong, T., J. McNames, M. Aboy, and B. Oken (2004), Averaged Lomb periodograms for non-uniform sampling, *Conf. Proc., IEEE Eng. Med Biol. Soc.*, *1*, 271–274.

Vadas, S. L. (2007), Horizontal and vertical propagation and dissipation of gravity waves in the thermosphere from lower atmospheric and thermospheric sources, *J. Geophys. Res.*, *112*, A06305, doi:10.1029/2006JA011845.

Vadas, S. L., H.-L. Liu, and R. S. Lieberman (2014), Numerical modeling of the global changes to the thermosphere and ionosphere from the dissipation of gravity waves from deep convection, *J. Geophys. Res. Space Physics*, *119*, 7762–7793, doi:10.1002/2014JA020280.

Walterscheid, R. L., G. Schubert, and J. Straus (1987), A dynamical-chemical model of wave-driven fluctuations in the OH nightglow, *J. Geophys. Res.*, *92*, 1241–1254, doi:10.1029/JA092iA02p01241.

Welch, P. D. (1967), The use of fast Fourier transform for the estimation of power spectra: A method based on time averaging over short, modified periodograms, *IEEE Trans. Audio Electroacoust.*, *15*(2), 70–73, doi:10.1109/TAU.1967.1161901.

Wright, J. W., and M. L. V. Pitteway (1979), Real-time data acquisition and interpretation capabilities of the Dynasonde: 1. Data acquisition and real-time display, *Radio Sci.*, *14*(5), 815–825, doi:10.1029/RS014i005p00815.

Wright, J. W., and M. L. V. Pitteway (1982), Data processing for the Dynasonde: The Dopplionogram, *J. Geophys. Res.*, *87*(A3), 1589–1598, doi:10.1029/JA087iA03p01589.

Wright, J. W., A. K. Paul, and M. L. V. Pitteway (1980), On the accuracy and interpretation of Dynasonde virtual height measurements, *Radio Sci.*, *15*(3), 617–626, doi:10.1029/RS015i003p00617.

Wright, J. W., and M. L. V. Pitteway (1999), A new data acquisition concept for digital ionosondes: Phase-based echo recognition and real-time parameter estimation, *Radio Sci.*, *34*(4), 871–882, doi:10.1029/1999RS900039.

Yigit, E., A. S. Medvedev, A. D. Aylward, P. Hartogh, and M. J. Harris (2009), Modeling the effects of gravity wave momentum deposition on the general circulation above the turbopause, *J. Geophys. Res.*, *114*, D07101, doi:10.1029/2008JD011132.

Zabotin, N. A., J. W. Wright, and G. A. Zhbankov (2006), NeXtYZ: Three-dimensional electron density inversion for dynasonde ionograms, *Radio Sci.*, *41*, RS6S32, doi:10.1029/2005RS003352.

Zhou, Q. H., M. P. Sulzer, and C. A. Tepley (1997), An analysis of tidal and planetary waves in the neutral winds and temperature observed at low-latitude *E* region heights, *J. Geophys. Res.*, *102*, 11,491–11,505, doi:10.1029/97JA00440.